INTERNATIONAL RESEARCH JOURNAL OF PHARMACY
www.irjponline.com
ISSN 2230 – 8407

Research Article

MICROWAVE ASSISTED SYNTHESIS AND MOLECULAR MODELING STUDIES OF SOME NOVEL POLO-LIKE KINASE 1 INHIBITORS AS ANTICANCER AND ANTI-INFLAMMATORY AGENTS

Ganesh K. Dhikale [1]*, Ramesh L. Sawant [2], Mahesh R. Dumbare [1]
[1] Department of Pharmaceutical Chemistry, Maratha Vidya Prasarak Samaj's College of Pharmacy, Gangapur Road, Nashik, Maharashtra, India
[2] Department of Pharmaceutical Chemistry and PG Studies, Dr. Vithalrao Vikhe Patil Foundation's College of Pharmacy, Post MIDC, Vilad Ghat, Ahmednagar, Maharashtra, India
*Corresponding Author Email: ganeshdhikale30987@gmail.com

Article Received on: 09/03/20 Approved for publication: 02/04/20

DOI: 10.7897/2230-8407.110442

ABSTRACT

A series of 1, 3-thiazolidin-4-one analogues were synthesized using microwave and structurally characterized by various spectroscopic techniques and elemental analysis. All synthesized compounds were screened for anticancer activity by sulforhodamine B (SRB) assay while *in vitro* anti-inflammatory activity was by inhibition of albumin denaturation technique. The compounds 5j, 5k, 5l, 5m, 5n were found to show significant anticancer and *in vitro* anti-inflammatory activity. Furthermore, molecular modelling studies of all molecules (5a-5s) were performed using V Life MDS software. Based on this it is observed that, compound 5m shows more stable complex with Polo-like kinase 1 by forming hydrogen bond and hydrophobic interactions. Finally it is concluded that, 1, 3-thiazolidin-4-one analogues shows anticancer and anti-inflammatory activity possibly because of inhibition of Polo-like kinase 1.

Keywords: 1, 3 – thiazolidin – 4 – one, Anti-cancer activity, Anti-inflammatory activity, Molecular Modeling, Polo-like kinase 1.

INTRODUCTION

Cancer is a group of cells which display uncontrolled growth, invasion and sometimes metastasis. During cancer progression inflammation occur via improper functioning of polo-like kinase (PLK1). Polo-like kinases plays a key role in cell cycle processes such as cell division and checkpoint regulation of mitosis. Polo-like kinase 1 controls various critical steps in M phase of cell cycle, including initiation with entry into mitosis nuclear envelope breakdown and bipolar spindle formation, chromosome separation at anaphase, centrosome maturation, sister chromatid splitting, activation of the anaphase-promoting complex, mitotic exit and the process of cytokinesis[1-3]. The level of PLK1 expression has prognostic value for predicting outcomes in patients with several cancers, like non-small cell lung cancer, squamous cell carcinomas of the head and neck, breast, melanomas, oropharyngeal, ovarian and endometrial carcinomas. The importance of PLK1 as a measure of tumor aggressiveness seems to come from its different functions during mitotic progression, particularly its role in the G2/M transition (phosphorylation of cyclin B1, a component of the mitosis-promoting factor)[4-5]. Also, PLK1 activates the Nuclear Factor kappa-light-chain-enhancer of activated B cells (NF-κB) protein which fuels inflammation through cyclooxygenase-2 (COX-2) enzymes and interleukins[6].

In US patent different analogues of thiazolidinones (1) have reported, use as inhibitors of PLK for treating various diseases including cancer[7]. Klaus Strebhardt has reported structure of ZK-thiazolidinone (2), an ATP competitive inhibitor with high selectivity for PLK 1 in a panel of 93 serine/threonine and tyrosine kinases[8]. Based on this study we have designed, synthesized and screened PLK1 inhibitors as an anticancer and anti-inflammatory.

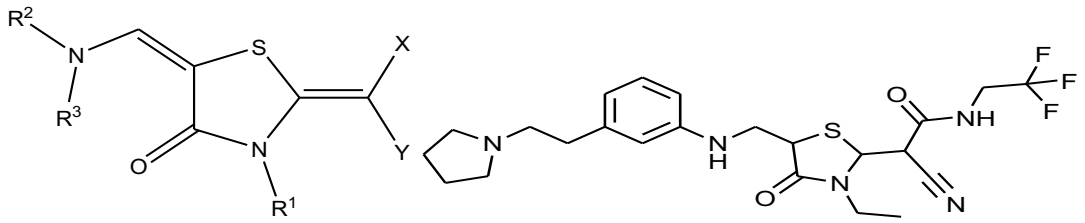

1 2

MATERIALS AND METHODS

All reagents and solvents of laboratory grade were used for synthesis. Melting points of all synthesized compounds were determined using Veego electronic (VMP-D) apparatus in an open capillary tube and are uncorrected. The structures of the title compounds were confirmed on the basis of spectral data. The IR spectra were recorded on a Jasco FTIR 4100 spectrophotometer. ^{1}H NMR spectra were recorded on a Varian-NMR-mercury YH-300 spectrometer using $CDCl_3$ as solvent with TMS as an internal standard. Mass spectra were recorded on an LC-MS Thermofinigan spectrometer. Reactions were monitored by silica gel G plate using suitable solvent system.

General Procedure for the synthesis of various N-(4-oxo-2-phenyl-1, 3-thiazolidin-3-yl) benzamides

The microwave assisted synthesis of compounds **5a–5s** followed the general pathway involved in following steps:

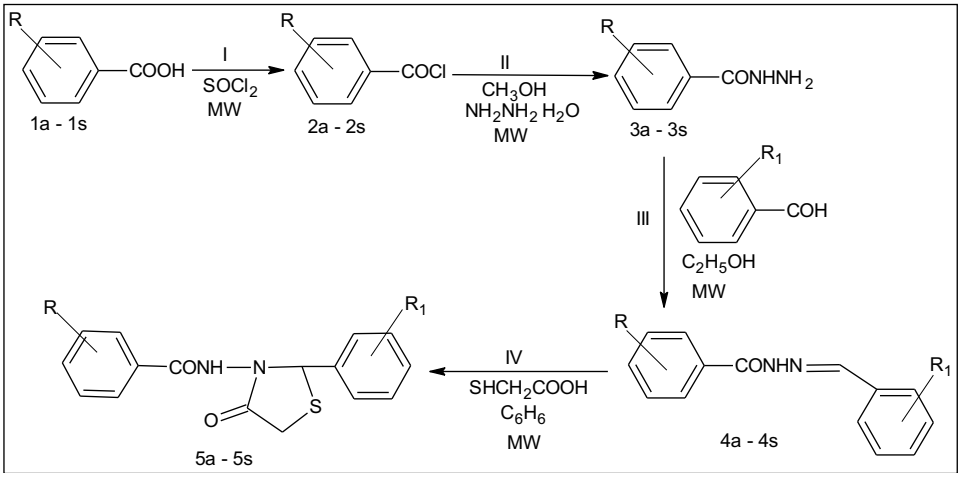

Reagent and condition: (I) Thionyl Chloride, MW; (II) Methanol, Hydrazine Hydrate, MW; (III) Aromatic Aldehyde, Ethanol, MW; (IV) Thioglycolic Acid, Benzene, MW[9-13]

The substituted benzoic acids (1a-1s) were treated with equimolar thionyl chloride to get the corresponding acid chlorides (2a-2s) which in turn were reacted with equimolar hydrazine hydrate to get the corresponding acid hydrazides (3a-3s). The reaction of hydrazides with different substituted benzaldehydes gave the corresponding benzylidene hydrazides (4a-4s), after treatment with thioglycolic acid gave the corresponding substituted N-(4-oxo-2-phenyl-1, 3-thiazolidin-3-yl) benzamides (5a–5s).

Characterization data of compounds

N-(4-oxo-2-phenyl-1,3-thiazolidin-3-yl)benzamide (5a)

IR (KBr*v* cm^{-1}) : 3248 (NH), 3050 (Ar CH), 1680, 1724 (C=O), 1527 (C=C), 724 (C-S). ^{1}H NMR (300 MHz, $CDCl_3$, δ ppm): 9.327 (s, 1H, CONH), 8.720 (s, 1H, NCHS), 7.609-7.898 (m, 5H, C_6H_5), 7.262-7.498 (m, 5H, C_6H_5), 3.094 (s, 2H, SCH_2). MS, *m/z* (M+1): 299. Anal. Calcd. for $C_{16}H_{14}N_2O_2S$: C,64.41; H, 4.73; N, 9.39. Found: C, 64.52; H, 4.81; N, 9.42.

N-{2-[4-(dimethylamino)phenyl]-4-oxo-1,3-thiazolidin-3-yl}benzamide (5b)

IR (KBr*v* cm^{-1}): 3310(NH), 3060 (Ar CH), 1667, 1745 (C=O), 1542 (C=C), 748 (C-S). ^{1}H NMR (300 MHz, $CDCl_3$, δ ppm): 9.264 (s, 1H, CONH), 8.720 (s, 1H, NCHS), 7.876-8.420 (m, 4H, C_6H_4), 7.262-7.610 (m, 5H, C_6H_5), 3.701 (s, 6H, $N(CH_3)_2$, 3.094 (s, 2H, SCH_2). MS, *m/z* (M+1): 342. Anal. Calcd. for $C_{18}H_{19}N_3O_2S$: C,63.32; H, 5.61; N, 12.31. Found: C, 63.44; H, 5.72; N, 12.39.

N-[2-(4-nitrophenyl)-4-oxo-1,3-thiazolidin-3-yl]benzamide (5c)

IR (KBr*v* cm^{-1}): 3270 (NH), 3080 (Ar CH),1686, 1732 (C=O), 1558 (C=C), 1546 (Ar-NO_2), 737 (C-S).^{1}H NMR (300 MHz, $CDCl_3$, δ ppm): 9.217 (s, 1H, CONH), 8.752 (s, 1H, NCHS), 7.588-7.896 (m, 4H, C_6H_4), 7.268-7.525 (m, 5H, C_6H_5), 3.092 (s, 2H, SCH_2). MS, *m/z* (M+1): 344. Anal. Calcd. for $C_{16}H_{13}N_3O_4S$: C,55.97; H, 3.82; N, 12.24. Found: C, 56.04; H, 3.95; N, 12.13.

N-[2-(4-chlorophenyl)-4-oxo-1,3-thiazolidin-3-yl]benzamide (5d)

IR (KBr*v* cm^{-1}): 3278(NH), 3040 (Ar CH), 1675, 1734 (C=O), 1582 (C=C), 868 (C-Cl), 728 (C-S). ^{1}H NMR (300 MHz, $CDCl_3$, δ ppm): 9.347 (s, 1H, CONH), 8.729 (s, 1H, NCHS), 7.896-8.492 (m, 4H, C_6H_4), 7.254-7.428 (m, 5H, C_6H_5), 3.086 (s, 2H, SCH_2). MS, *m/z* (M+1): 333. Anal. Calcd. for $C_{16}H_{13}N_2O_2SCl$: C,57.74; H, 3.94; N, 8.42. Found: C, 57.86; H, 3.98; N, 8.54.

N-[2-(4-methoxyphenyl)-4-oxo-1,3-thiazolidin-3-yl]benzamide (5e)

IR (KBr*v* cm^{-1}): 3257 (NH), 3096 (Ar CH), 1674, 1712 (C=O), 1574 (C=C), 1257 (C-O), 696 (C-S).^{1}H NMR (300 MHz, $CDCl_3$, δ ppm): 9.220 (s, 1H, CONH), 8.762 (s, 1H, NCHS), 7.845-8.176 (m, 4H, C_6H_4), 7.265-7.534 (m, 5H, C_6H_5), 3.638 (s, OCH_3), 3.115 (s, 2H, SCH_2). MS, *m/z* (M+1): 329. Anal. Calcd. for $C_{17}H_{16}N_2O_3S$: C,62.18; H, 4.91; N, 8.53. Found: C, 62.29; H, 4.99; N, 8.63.

N-(4-oxo-2-phenyl-1,3-thiazolidin-3-yl)-4-nitrobenzamide (5f)

IR (KBr*v* cm^{-1}): 3275 (NH), 3078 (Ar CH),1670, 1756 (C=O), 1574 (C=C), 1552 (Ar-NO_2), 732 (C-S). ^{1}H NMR (300 MHz, $CDCl_3$, δ ppm): 9.224 (s, 1H, CONH), 8.754 (s, 1H, NCHS), 7.682-7.920 (m, 4H, C_6H_4), 7.278-7.486 (m, 5H, C_6H_5), 3.152 (s,

2H, SCH_2). MS, *m/z* (M+1): 344. Anal. Calcd. for $C_{16}H_{13}N_3O_4S$: C,55.97; H, 3.82; N, 12.24. Found: C, 55.91; H, 3.71; N, 12.34.

N-{2-[4-(dimethylamino)phenyl]-4-oxo-1,3-thiazolidin-3-yl}-4-nitrobenzamide (5g)

IR (KBr*ν* cm^{-1}): 3294 (NH), 3090 (Ar CH), 1685, 1728 (C=O), 1558 (C=C), 1532 (Ar-NO_2), 727 (C-S).^{1}H NMR (300 MHz, $CDCl_3$, δ ppm): 9.318 (s, 1H, CONH), 8.802 (s, 1H, NCHS), 7.862-8.357 (m, 4H, C_6H_4), 7.447-7.720 (m, 4H, C_6H_4), 3.851 (s, 6H, $N(CH_3)_2$, 3.296 (s, 2H, SCH_2). MS, *m/z* (M+1): 387. Anal. Calcd. for $C_{18}H_{18}N_4O_4S$: C,55.95; H, 4.70; N, 14.50. Found: C, 54.88; H, 4.63; N, 14.62.

N-[2-(4-chlorophenyl)-4-oxo-1,3-thiazolidin-3-yl]-4-nitrobenzamide (5h)

IR (KBr*ν* cm^{-1}): 3248 (NH), 3085 (Ar CH),1690, 1754 (C=O), 1538 (C=C), 1568 (Ar-NO_2), 912 (C-Cl), 738 (C-S).^{1}H NMR (300 MHz, $CDCl_3$, δ ppm): 9.364 (s, 1H, CONH), 8.694 (s, 1H, NCHS), 7.884-8.428 (m, 4H, C_6H_4), 7.385-7.678 (m, 4H, C_6H_4), 3.195 (s, 2H, SCH_2). MS, *m/z* (M+1): 378. Anal. Calcd. for $C_{16}H_{12}N_3O_4SCl$: C,50.87; H, 3.20; N, 11.12. Found: C, 50.93; H, 3.25; N, 11.18.

N-[2-(4-methoxyphenyl)-4-oxo-1,3-thiazolidin-3-yl]-4-nitrobenzamide (5i)

IR (KBr*ν* cm^{-1}): 3290 (NH), 3082 (Ar CH), 1676, 1742 (C=O), 1574 (C=C), 1550 (Ar-NO_2), 1219 (C-O), 706 (C-S). ^{1}H NMR (300 MHz, $CDCl_3$, δ ppm): 9.384 (s, 1H, CONH), 8.783 (s, 1H, NCHS), 7.852-8.268 (m, 4H, C_6H_4), 7.416-7.694 (m, 4H, C_6H_4), 3.586 (s, OCH_3), 3.160 (s, 2H, SCH_2). MS, *m/z* (M+1): 374. Anal. Calcd. for $C_{17}H_{15}N_3O_5S$: C,54.68; H, 4.05; N, 11.25. Found: C, 54.81; H, 4.17; N, 11.31.

N-(4-oxo-2-phenyl-1,3-thiazolidin-3-yl)-2-hydroxybenzamide (5j)

IR (KBr*ν* cm^{-1}): 3257 (NH), 3087 (Ar CH), 3357 (OH), 1688, 1734 (C=O), 1527 (C=C), 718 (C-S). ^{1}H NMR (300 MHz, $CDCl_3$, δ ppm): 10.076 (s, 1H, OH), 9.238 (s, 1H, CONH), 8.780 (s, 1H, NCHS), 7.965-8.482 (m, 4H, C_6H_4), 7.542-7.876 (m, 5H, C_6H_5), 3.142 (s, 2H, SCH_2). MS, *m/z* (M+1): 315. Anal. Calcd. for $C_{16}H_{14}N_2O_3S$: C,61.13; H, 4.49; N, 8.91. Found: C, 61.26; H, 4.61; N, 8.81.

N-{2-[4-(dimethylamino)phenyl]-4-oxo-1,3-thiazolidin-3-yl}-2-hydroxybenzamide (5k)

IR (KBr*ν* cm^{-1}): 3348 (NH), 3094 (Ar CH), 3312 (OH), 1674, 1730 (C=O), 1554 (C=C), 735(C-S). ^{1}H NMR (300 MHz, $CDCl_3$, δ ppm): 10.094 (s, 1H, OH), 9.412 (s, 1H, CONH), 8.652 (s, 1H, NCHS), 7.718-8.396 (m, 4H, C_6H_4), 7.384-7.684 (m, 4H, C_6H_4), 3.754 (s, 6H, $N(CH_3)_2$, 3.492 (s, 2H, SCH_2). MS, *m/z* (M+1): 358. Anal. Calcd. for $C_{18}H_{19}N_3O_3S$: C,60.49; H, 5.36; N, 11.76. Found: C, 60.56; H, 5.49; N, 11.85.

N-[2-(4-nitrophenyl)-4-oxo-1,3-thiazolidin-3-yl]-2-hydroxybenzamide (5l)

IR (KBr*ν* cm^{-1}): 3267 (NH), 3052 (Ar CH), 3327 (OH), 1668, 1719 (C=O), 1584 (C=C), 1542(Ar-NO_2), 698 (C-S). ^{1}H NMR (300 MHz, $CDCl_3$, δ ppm): 10.282 (s, 1H, OH), 9.387 (s, 1H, CONH), 8.646 (s, 1H, NCHS), 7.768-7.996 (m, 4H, C_6H_4), 7.489-7.632 (m, 4H, C_6H_4), 3.282 (s, 2H, SCH_2). MS, *m/z* (M+1): 360. Anal. Calcd. for $C_{16}H_{13}N_3O_5S$: C,53.48; H, 3.65; N, 11.69. Found: C, 53.61; H, 3.53; N, 11.72.

N-[2-(4-chlorophenyl)-4-oxo-1,3-thiazolidin-3-yl]-2-hydroxybenzamide (5m)

IR (KBr*ν* cm^{-1}): 3385 (NH), 3058 (Ar CH), 3310 (OH), 1624, 1752 (C=O), 1512 (C=C), 918 (C-Cl), 724 (C-S). ^{1}H NMR (300 MHz, $CDCl_3$, δ ppm): 10.176 (s, 1H, OH), 9.385 (s, 1H, CONH), 8.468 (s, 1H, NCHS), 7.612-7.892 (m, 4H, C_6H_4), 7.342-7.514 (m, 4H, C_6H_4), 3.252 (s, 2H, SCH_2). MS, *m/z* (M+1): 349. Anal. Calcd. for $C_{16}H_{13}N_2O_3SCl$: C,55.09; H, 3.76; N, 8.03. Found: C, 55.23; H, 3.83; N, 7.95.

N-[2-(4-methoxyphenyl)-4-oxo-1,3-thiazolidin-3-yl]-2-hydroxybenzamide (5n)

IR (KBr*ν* cm^{-1}): 3250 (NH), 3040 (Ar CH), 3306 (OH), 1698, 1736 (C=O), 1534 (C=C), 1214 (C-O), 692 (C-S). ^{1}H NMR (300 MHz, $CDCl_3$, δ ppm) : 10.147 (s, 1H, OH), 9.412 (s, 1H, CONH), 8.582 (s, 1H, NCHS), 7.758-8.192 (m, 4H, C_6H_4), 7.462-7.624 (m, 4H, C_6H_4), 3.716 (s, OCH_3), 3.292 (s, 2H, SCH_2). MS, *m/z* (M+1): 345. Anal. Calcd. for $C_{17}H_{16}N_2O_4S$: C,59.29; H, 4.68; N, 8.13. Found: C, 59.38; H, 4.74; N, 8.08.

N-(4-oxo-2-phenyl-1,3-thiazolidin-3-yl)-2-chlorobenzamide (5o)

IR (KBr*ν* cm^{-1}): 3336(NH), 3068 (Ar CH), 1682, 1724 (C=O), 1542 (C=C), 864 (C-Cl), 738 (C-S). ^{1}H NMR (300 MHz, $CDCl_3$, δ ppm): 9.362 (s, 1H, CONH), 8.658 (s, 1H, NCHS), 7.978-8.296 (m, 4H, C_6H_4), 7.264-7.428 (m, 5-H, C_6H_5), 3.345 (s, 2H, SCH_2). MS, *m/z* (M+1): 333. Anal. Calcd. for $C_{16}H_{13}N_2O_2SCl$: C,57.74; H, 3.94; N, 8.44. Found: C, 57.83; H, 3.82; N, 8.48.

N-{2-[4-(dimethylamino)phenyl]-4-oxo-1,3-thiazolidin-3-yl}-2-chlorobenzamide (5p)

IR (KBr*ν* cm^{-1}): 3357(NH), 3050 (Ar CH), 1658, 1740 (C=O), 1514 (C=C), 804 (C-Cl), 726 (C-S).^{1}H NMR (300 MHz, $CDCl_3$, δ ppm): 9.478 (s, 1H, CONH), 8.772 (s, 1H, NCHS), 7.984-8.296 (m, 4H, C_6H_4), 7.418-7.612 (m, 4H, C_6H_4), 3.612 (s, 6H, $N(CH_3)_2$, 3.252 (s, 2H, SCH_2). MS, *m/z* (M+1): 376. Anal. Calcd. for $C_{18}H_{18}N_3O_2SCl$: C,57.52; H, 4.83; N, 11.18. Found: C, 57.66; H, 4.91; N, 11.12

N-[2-(4-nitrophenyl)-4-oxo-1,3-thiazolidin-3-yl]-2-chlorobenzamide (5q)

IR (KBr*ν* cm^{-1}): 3248 (NH), 3060 (Ar CH), 1690, 1735 (C=O), 1520 (C=C), 1542 (Ar-NO_2), 856 (C-Cl), 718 (C-S).^{1}H NMR (300 MHz, $CDCl_3$, δ ppm): 9.587 (s, 1H, CONH), 8.452 (s, 1H, NCHS), 7.924-8.216 (m, 4H, C_6H_4), 7.342-7.514 (m, 4H, C_6H_4), 3.426 (s, 2H, SCH_2). MS, *m/z* (M+1): 378. Anal. Calcd. for $C_{16}H_{12}N_3O_4SCl$: C,50.87; H, 3.20; N, 11.12. Found: C, 50.96; H, 3.27; N, 11.21.

N-[2-(4-chlorophenyl)-4-oxo-1,3-thiazolidin-3-yl]-2-chlorobenzamide (5r)

IR (KBr*ν* cm^{-1}): 3318 (NH), 3075 (Ar CH), 1667, 1716 (C=O), 1522 (C=C),952 (C-Cl), 735 (C-S).^{1}H NMR (300 MHz, $CDCl_3$, δ ppm): 9.612 (s, 1H, CONH), 8.629 (s, 1H, NCHS), 7.984-8.264 (m, 4H, C_6H_4), 7.434-7.604 (m, 4H, C_6H_4), 3.246 (s, 2H, SCH_2). MS, *m/z* (M+1): 368. Anal. Calcd. for $C_{16}H_{12}N_2O_2SCl_2$: C,52.33; H, 3.29; N, 7.63. Found: C, 52.25; H, 3.33; N, 7.57.

N-[2-(4-methoxyphenyl)-4-oxo-1,3-thiazolidin-3-yl]-2-chlorobenzamide (5s)

IR (KBr*v* cm^{-1}): 3292 (NH), 3024 (Ar CH), 1692, 1728 (C=O), 1534 (C=C),1226 (C-O), 870 (C-Cl), 717 (C-S).^{1}H NMR (300 MHz, $CDCl_3$, δ ppm): 9.487 (s, 1H, CONH), 8.342 (s, 1H, NCHS), 7.938-8.276 (m, 4H, C_6H_4), 7.439-7.648 (m, 4H, C_6H_4), 3.648 (s, OCH_3), 3.269 (s, 2H, SCH_2). MS, *m/z* (M+1): 363. Anal. Calcd. for $C_{17}H_{15}N_2O_3SCl$: C,56.27; H, 4.17; N, 7.72. Found: C, 56.13; H, 4.09; N, 7.81.

Anticancer activity

The cell lines MCF7 were grown in RPMI 1640 medium containing 10% fetal bovine serum and 2 mM L-glutamine. The cells were inoculated into 96 well micro titer plates in 90 µl plating densities, depending on the doubling time of individual cell lines. After cell inoculation, the micro titer plates were incubated at 37° C, 5% CO_2, 95% air and 100% relative humidity for 24 hours prior to addition of experimental drugs (5a – 5s).

After 24 hours, one plate of each cell line was fixed *in situ* with trichloro acetic acid (TCA) to represent a measurement of the cell population for each cell line at the time of drug addition, time zero (Tz). Experimental drugs were solubilized in appropriate solvent at 400-fold the desired final maximum test concentration and stored frozen prior to use. At the time of drug addition, an aliquot of frozen concentrate was thawed and diluted to 10 times the desired final maximum test concentration with complete medium containing test article at a concentration of 10^{-3}. Additional three, 10-fold serial dilutions were made to provide a total of four drug concentrations plus control. Aliquots of 10 µl of these different drug dilutions were added to the appropriate micro titer wells already containing 90 µl of medium resulting in the required final drug concentrations.

Endpoint measurement

After compound addition, plates were incubated at standard conditions for 48 hours and assay was terminated by the addition of cold TCA. Cells were fixed *in situ* by the gentle addition of 50 µl of cold 30% (w/v) TCA (final concentration, 10% TCA) and incubated for 60 minutes at 4°C. The supernatant was discarded; the plates were washed five times with tap water and air dried. Sulforhodamine B (SRB) solution (50 µl) at 0.4% (w/v) in 1% acetic acid was added to each of the wells and plates were incubated for 20 minutes at room temperature. After staining, unbound dye was recovered and the residual dye was removed by washing five times with 1% acetic acid. The plates were air dried. Bound stain was subsequently eluted with 10 mM trizma base and the absorbance was read on an Elisa plate reader at a wavelength 540 nm with reference wavelength 690 nm.

Percent growth was calculated on a plate-by-plate basis for test wells relative to control wells. Using the six absorbance measurements [time zero (Tz), control growth (C) and test growth in the presence of drug at the four concentration levels (Ti)], the percentage growth was calculated at each of the drug concentration levels. Percentage growth inhibition was calculated as:

[(Ti-Tz)/(C-Tz)] × 100 for concentrations for which Ti>/=Tz (Ti-Tz) positive or zero

[(Ti-Tz)/Tz] × 100 for concentrations for which Ti<Tz. (Ti-Tz) negative

The dose response parameters were calculated for each test article. Growth inhibition of 50 % (GI_{50}) was calculated from [(Ti-Tz)/(C-Tz)] × 100 = 50 which is the drug concentration resulting in a 50% reduction in the net protein increase (as measured by SRB staining) in control cells during the drug incubation. The drug concentration resulting in total growth inhibition (TGI) was calculated from Ti = Tz. The LC_{50} (concentration of drug resulting in a 50% reduction in the measured protein at the end of the drug treatment as compared to that at the beginning) indicating a net loss of cells following treatment is calculated from [(Ti-Tz)/Tz] × 100 = -50.

Values were calculated for each of these three parameters if the level of activity was reached; however, if the effect was not reached or was exceeded, the values for that parameter were expressed as greater or less than the maximum or minimum concentration tested[14–15].

***In vitro* Anti-inflammatory activity**

The synthesized compounds (5a – 5s) were screened for anti-inflammatory activity by using inhibition of albumin denaturation technique. The diclofenac was used as standard drug. Both standard and test drugs (5a – 5s) were dissolved in minimum amount of dimethyl formamide (DMF) and diluted with phosphate buffer (0.2 M, pH 7.4). Final concentration of DMF in all solutions was less than 2.5%. Test solution (1 ml) containing different concentrations of drug was mixed with 1 ml of 1% mM albumin solution in phosphate buffer and incubated at 27 ± 1^0C in BOD incubator for 15 min. Denaturation was induced by keeping the reaction mixture at 60 ± 10^0C on water bath for 10 min. After cooling, the turbidity was measured at wavelength 660 nm using double beam UV-visible spectrophotometer. The percentage inhibition of denaturation was calculated from control where no drug was added. Each experiment was done in duplicate and average was taken. The % inhibition can be calculated by using the formula; % of inhibition = 100 × ((Vc / Vt) - 1) where, Vt mean absorbance value of test group and Vc indicates absorbance value of control group. From percentage inhibition the 50% Inhibitory Concentration (IC_{50}) was calculated[16-17].

Molecular docking

Protein Preparation

The X-ray crystallographic structure of human PLK1 (PDB ID 1Q4K X-ray resolution of 2.3 A^0) in complex with phospo-peptide was obtained from the protein data bank. Crystallographic protein structure downloaded from protein data bank contains various potential problems which must be resolved. These issues involved removal of water and other co-crystal ligands, addition of hydrogen atoms and assigning correct charges to protein structures. Preparation of protein structures for docking purpose were performed using VLife Molecular Design Suite (VlifeMDS, VLife Technologies, Pune, MS).

Ligands Preparation

The structures of substituted N-(4-oxo-2-phenyl-1, 3-thiazolidin-3-yl) benzamide (5a – 5s) were generated using the 2D Draw tool of the V Life MDS. The 3D structures were prepared for docking by adding hydrogen atoms and energy minimized using force field MMFF with RMSD gradient of 0.01 kcal/mol A. Flexible Docking was performed for all these ligands as confirmations of ligands also generated and dock in this module of molecular docking. All these steps were carried out using V Life MDS.

Docking Study

The following molecular docking study was carried out with an aim to rationalise the background for synthesizing the different 1,3-thiazolidin-4-ones molecules with respect to their inhibitory activity towards PLK1 in the light of designing novel promising anticancer agents. The active site used for docking was determined on the basis of hydrophobic nature of the cavity. Most hydrophobic cavity was selected for molecular docking. The software V Life MDS has been utilized for carrying out the molecular docking. Docking score was used as the dock scoring function. All the ligands were docked in to the binding site of PLK1. Analysis of the docking results was based on both the docking score as well as the binding interactions with active site residues[18].

Quantitative structure activity relationship (QSAR)

The anti-inflammatory activity shown that novel compounds (5a-5s) have been fulfilling criterion for QSAR study, we proceed accordingly.

Biological Activity Data

A data set of 19 compounds (5a – 5s) of substituted N-(4-oxo-2-phenyl-1, 3-thiazolidin-3-yl) benzamide for *in vitro* anti-inflammatory activity was used for the present QSAR study. There is sufficient range of the biological activity in the selected series of these derivatives (Table 1). The biological activity of these derivatives has been measured in terms of inhibitory activity pIC50. In this work, we describe 2DQSAR and3D-QSAR study for N-(4-oxo-2-phenyl-1, 3-thiazolidin-3-yl) benzamide analogue in order to compare the information obtained from 2D and 3D arrangements of atoms in the molecules with classical QSAR and extract more information in terms of steric and electrostatic, hydrophobic properties from 3D-QSAR methods.

Geometry Optimization

Molecular modelling and calculation of various parameters required for QSAR model development were performed using V Life MDS. Structures of the molecules (5a – 5s) were drawn using the 2D builder module of V Life MDS. All molecules were converted to 3D structures[18] and batch optimized for the minimization of energies using Merck molecular force field (MMFF) followed by considering distance-dependent dielectric constant of 1.0 and convergence criterion of 0.01 kcal/mol A[19]. Most stable structure for each compound was generated and used for calculating various physicochemical descriptors like thermodynamic, steric, and electronic values of descriptors.

Creation of Training and Test Set

The total set is randomly divided into two subsets: a training set for the dramatization of QSAR model and a test set for validating the quality of QSAR model. Selection of the training and the test set for the QSAR model was done by considering the fact that the test set compounds should represent structural diversity and a range of biological activities similar to that of the training set. Molecules were divided into training and test data set comprising of 15 and 04 molecules respectively.

2D-QSAR Studies

All the calculated 2D descriptors were considered as independent variable and biological activity as dependent variable. The energy-minimized geometry was used for the calculation of the various 2D descriptors Individual, Chi, ChiV, Path count, Cluster, Path cluster, Kappa, Element Count, Estate number, Estate contribution, Semi empirical, Polar surface area, and Alignment independent and was considered as independent variables in this study[20].

Alignment of molecules

Molecular alignment is a crucial step in 3D-QSAR study to obtain meaningful results. This method is based on moving of molecules in 3D space, which is related to the conformational flexibility of molecules. The goal is to obtain optimal alignment between the molecular structures necessary for ligand–receptor interactions. All molecules in the data set were aligned by template-based method where a template is built by considering common substructures in the series. A structure without any substitution is chosen as a template molecule on which other molecules in the series are aligned. The structure of N-(4-oxo-2-phenyl-1, 3-thiazolidin-3-yl) benzamide(5a) template is shown in Figure 1. The aligned view of 1,3-thiazolidin-4-ones/ N-(4-oxo-2-phenyl-1, 3-thiazolidin-3-yl) benzamide analogues is presented in Figure 2.

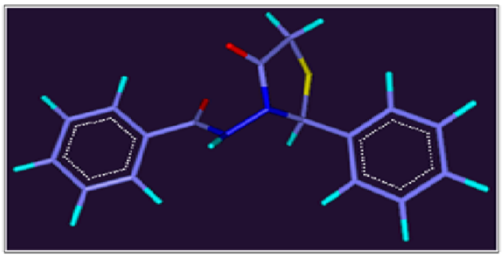

Figure 1: Template molecule (stick model)

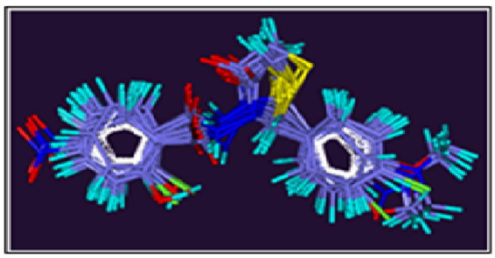

Figure 2: Alignment of compounds on template molecule (stick model)

Computation of steric and electrostatic fields

The aligned biologically active conformations of N-(4-oxo-2-phenyl-1, 3-thiazolidin-3-yl) benzamides (5a – 5s) are used for the calculation of molecular fields. Molecular fields are the steric and electrostatic interaction energies, used to formulate a relationship between steric and electrostatic properties together with the biological activities of compounds. Each conformation is taken in turn, and the molecular fields around it are calculated. This is done by generating three-dimensional rectangular grids around the molecule and calculating the interaction energy between the molecule and probe group placed at each grid point. Steric and electrostatic fields are computed at each grid point considering MMFF charges. Methyl probe of charge +1 with 10.0

kcal/mole electrostatic and 30.0 kcal/mole steric cut off were used for fields generation. A value of 1.0 is assigned to the distance-dependent dielectric constant. Steric and electrostatic field descriptors were calculated using Lennard–Jones and Coulomb potentials.

In the present study, molecular field analysis coupled with partial least squares (PLS) was applied to obtain a 3D-QSAR model based on steric and electrostatic descriptors. Since multi coli neared among the computed descriptors may detrimentally affect the regression analysis, PLS is frequently used as the regression method in 3D-QSAR. The calculated steric and electrostatic field descriptors were used as independent variables and pIC50 values were used as dependent variables in PLS regression analysis to derive the 3D-QSAR models using V life MDS software. The internal predictability of the models was evaluated in terms of cross validated $q2$[21].

RESULT AND DISCUSSION

Microwave assisted synthesis of compounds 5a-5s along with their reaction time and physicochemical properties has been mentioned in Table 1. The structures of compounds (5a-5s) were confirmed by IR, NMR, mass spectral data and elemental analysis.

Table 1: Reaction Time and physicochemical properties of compounds (5a – 5s)

S. No.	Compound	R	R_1	Reaction Time	Molecular formula	% yield	M. P. (^{0}C)	R_f[a] Value
1.	**5a**	H	H	08	$C_{16}H_{14}N_2O_2S$	88.45	188-190	0.16
2.	**5b**	H	4-N$(CH_3)_2$	05	$C_{18}H_{19}N_3O_2S$	84.53	238-240	0.24
3.	**5c**	H	4-NO_2	06	$C_{16}H_{13}N_3O_4S$	78.18	202-204	0.20
4.	**5d**	H	4-Cl	09	$C_{16}H_{13}N_2O_2SCl$	86.54	218-220	0.18
5.	**5e**	H	4-OCH_3	08	$C_{17}H_{16}N_2O_3S$	92.34	196-198	0.27
6.	**5f**	4-NO_2	H	07	$C_{16}H_{13}N_3O_4S$	83.48	252-254	0.57
7.	**5g**	4-NO_2	4-N$(CH_3)_2$	05	$C_{18}H_{18}N_4O_4S$	90.64	154-156	0.68
8.	**5h**	4-NO_2	4-Cl	06	$C_{16}H_{12}N_3O_4SCl$	78.74	260-262	0.62
9.	**5i**	4-NO_2	4-OCH_3	08	$C_{17}H_{15}N_3O_5S$	80.22	245-247	0.76
10.	**5j**	2-OH	H	12	$C_{16}H_{14}N_2O_3S$	76.16	210-212	0.78
11.	**5k**	2-OH	4-N$(CH_3)_2$	07	$C_{18}H_{19}N_3O_3S$	78.34	230-232	0.85
12.	**5l**	2-OH	4-NO_2	05	$C_{16}H_{13}N_3O_5S$	88.32	124-132	0.83
13.	**5m**	2-OH	4-Cl	09	$C_{16}H_{13}N_2O_3SCl$	79.24	224-226	0.81
14.	**5n**	2-OH	4-OCH_3	06	$C_{17}H_{16}N_2O_4S$	81.46	215-217	0.91
15.	**5o**	2-Cl	H	11	$C_{16}H_{13}N_2O_2SCl$	78.28	148-150	0.31
16.	**5p**	2-Cl	4-N$(CH_3)_2$	06	$C_{18}H_{18}N_3O_2SCl$	85.61	78-80	0.40
17.	**5q**	2-Cl	4-NO_2	07	$C_{16}H_{12}N_3O_4SCl$	78.65	102-104	0.37
18.	**5r**	2-Cl	4-Cl	05	$C_{16}H_{12}N_2O_2SCl_2$	76.24	174-176	0.34
19.	**5s**	2-Cl	4-OCH_3	04	$C_{17}H_{15}N_2O_3SCl$	82.28	166-168	0.45

[a]Solvent System – benzene:ethyl acetate (2:3 v/v)

The anticancer activity of compounds (5a-5s) was determined by sulforhodamine (SRB) assay with MCF7 cell lines for breast cancer. Among these compounds 5j, 5k, 5l, 5m and 5n were found to be most active showing LC_{50}<0.1 µmoles comparable with adriamycin (ADR). The results of anticancer activity have been reported in Table 2.

Anti-inflammatory activity of compounds (5a-5s) was determined by inhibition of albumin denaturation technique. Amongst these5j, 5k, 5l, 5m and 5n have shown IC_{50} in range of 191.89-240.66 µg/ml as compared with diclofenac (IC_{50} 188.25 µg/ml). The results for anti-inflammatory activity have been reported in Table 2.

The docking of all compounds (5a-5s) and reference compounds adriamycin and diclofenac were performed with PLK1 (PDB code 1Q4K) using V Life MDS. The docking results have been reported in Table 2. The docking study shows that all compounds (5a-5s) have good interaction with PLK1. Among these compound 5m has highest dock score (-5.860344) indicating most stable drug-receptor complex with PLK1 by forming hydrogen bond interaction with LEU523, LEU525, VAL530 and GLN531 and hydrophobic interaction with MET377, HIS524, LEU525, GLY528, SER529 and VAL530 (Figure 3 A). Whereas adriamycin forms hydrogen bond interaction with VAL411, THR513, HIS524, GLY528, VAL530 and LEU543 and hydrophobic interaction with LEU374, MET377, TRP410, VAL411, LEU427, LEU511, ARG512, THR513, ILE522, LEU523, HIS524, LEU525, SER529, VAL530, GLN531, LEU543, PRO545, VAL587 and LEU590 (Figure 3 B) and diclofenac shows hydrogen bond interaction with VAL530 and hydrophobic interactions with MET377, HIS524, SER529, VAL530 and GLN531 (Figure 3 C)

Table 2: Anticancer, *In vitro* anti-inflammatory Activity and Molecular docking score of compounds (5a - 5s)

Compound	R	R_1	Anticancer Activity LC_{50} (µmoles)	Anti-inflammatory Activity IC_{50} (µg/ml)	Docking score (Kcal/mol)
5a	H	H	>100	278.94	-5.530135
5b	H	4-$N(CH_3)_2$	>100	253.74	-5.466703
5c	H	4-NO_2	>100	247.81	-5.557520
5d	H	4-Cl	>100	270.37	-5.757302
5e	H	4-OCH_3	>100	259.93	-5.245671
5f	4-NO_2	H	>100	277.81	-5.391098
5g	4-NO_2	4-$N(CH_3)_2$	97.2	261.62	-5.317842
5h	4-NO_2	4-Cl	>100	294.59	-5.642852
5i	4-NO_2	4-OCH_3	89.1	265.18	-5.302423
5j	2-OH	H	<0.1	240.66	-5.615132
5k	2-OH	4-$N(CH_3)_2$	<0.1	212.60	-5.606740
5l	2-OH	4-NO_2	<0.1	226.14	-5.503796
5m	2-OH	4-Cl	<0.1	191.89	-5.860344
5n	2-OH	4-OCH_3	<0.1	202.66	-5.342855
5o	2-Cl	H	82.9	287.04	-5.779104
5p	2-Cl	4-$N(CH_3)_2$	>100	257.73	-5.728557
5q	2-Cl	4-NO_2	80.1	272.75	-5.601307
5r	2-Cl	4-Cl	>100	262.18	-5.702049
5s	2-Cl	4-OCH_3	69.5	284.07	-5.400191
Adriamycin	-	-	<0.1	-	-5.885807
Diclofenac	-	-	-	188.25	-5.654936

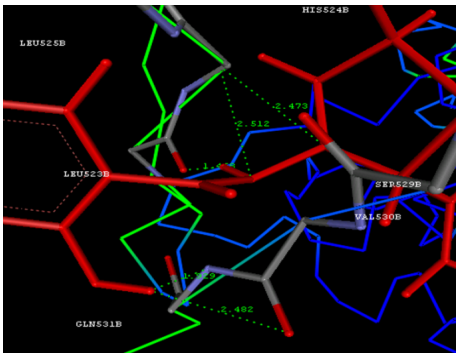

Figure 3 A: Binding pose of compound 5m and PLK1

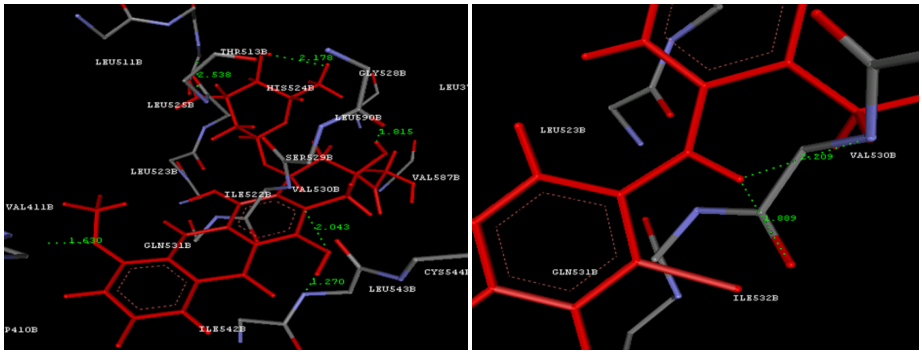

3 B: Binding pose of Adriyamycin and PLK1.C) Binding pose of Diclofenac and PLK1.

Furthermore, 2D and 3D QSAR analysis of compounds (5a - 5s) was also performed for *in vitro* anti-inflammatory activity.

2D QSAR

pIC_{50} = 2.5439–0.0103(±0.00014) Most +ve and –ve Potential Distance - 0.0091 (± 0.65422) SsOHE- index-0.0272 (± 0.36136) T_2_S_6
n = 15, r^2 = 0.8588, q^2 = 0.7506, F test = 36.4831.....**Model – 1**

Where,
n = number of molecules, r = square root of the multiple R-squared for regression, q = cross-validated r^2, F = statistic for the regression model

The model-1 indicates that the anti-inflammatory activity is dependent on Alignment Independent, Estate contribution and Electrostatic descriptors. The model-1 reveals that descriptor T_2_S_6 is negative contributor to activity which indicate the count of number of double bounded atoms (i.e. any double bonded atom, T_2) separated from sulfur atom by 6 bonds in a molecule require for activity. The next influencing descriptor is Most +ve and –ve Potential Distance which also negative contributor to the activity, suggesting that the distance between points having the highest value of +ve and highest value of –ve

electrostatic potential on van der Waals surface area of the molecule. The descriptor SsOHE-index is also negative contributor, indicating that the electrotopological state indices for number of –OH group connected with one single bond will determine the activity. The 2D descriptors, actual pIC_{50}, predicted pIC_{50} and residual values have been mentioned in Table 3.

Table 3: The 2D QSAR descriptors of model-1 with actual pIC_{50}, predicted pIC_{50} and residual value

Comp	Most +ve and -ve Potential Distance	SsOHE-index	T_2_S_6	Actual pIC_{50}	Predicted pIC_{50}	Residual
5a	5.012439	0	2	2.453425	2.437635	0.007876
5b	5.786705	0	2	2.445511	2.429634	-0.02525
5c	4.989913	0	3	2.404389	2.410645	-0.01653
5d	4.545887	0	2	2.394119	2.442457	-0.0105
5e	5.265601	0	2	2.431959	2.435019	-0.02016
5f*	5.606026	0	2	2.414856	2.431501	0.012247
5g	8.261361	0	2	2.443748	2.404061	0.013593
5h	4.567677	0	2	2.417654	2.442232	0.026986
5i*	4.676274	0	2	2.469218	2.441109	-0.01759
5j	4.535524	9.752719	2	2.381402	2.354012	0.02739
5k*	4.475258	9.830589	2	2.327543	2.353928	-0.02639
5l*	7.845589	9.771417	3	2.35437	2.292413	0.061957
5m	3.84362	9.787795	2	2.283039	2.360844	-0.07781
5n	8.442866	9.796504	2	2.306783	2.313235	-0.00645
5o	4.88296	0	2	2.457942	2.438973	0.018969
5p	7.911988	0	2	2.411165	2.407671	0.003494
5q	4.798298	0	3	2.435765	2.412626	0.023139
5r	4.863309	0	2	2.4186	2.439176	-0.02058
5s	4.718944	0	2	2.453425	2.440668	0.012757

* Test set compound

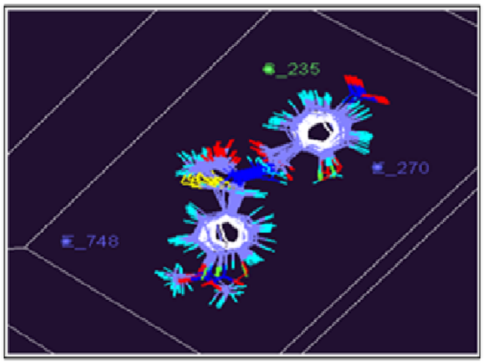

Figure 4: Grid point interaction for model-2

Table 4: The 3D QSAR descriptors of model-2 with actual pIC_{50}, predicted pIC_{50} and residual value

Comp	E_270	S_235	E_748	Actual pIC_{50}	Predicted pIC_{50}	Residual
5a	10	0.598948	0.197193	2.453425	2.447743	-0.00223
5b*	9.462493	2.901299	0.339897	2.445511	2.447109	-0.04272
5c	10	1.824706	-0.09258	2.404389	2.412291	-0.01817
5d	2.939906	-0.4008	0.088766	2.394119	2.413546	0.018413
5e	10	7.635483	0.386703	2.431959	2.428063	-0.01321
5f	6.633188	1.386919	0.293554	2.414856	2.439208	0.00454
5g	10	6.255457	0.351944	2.443748	2.432161	-0.01451
5h	10	1.665538	0.285143	2.417654	2.450635	0.018583
5i*	10	4.105776	0.486819	2.469218	2.457298	-0.03377
5j	-1.03802	-0.31208	0.008599	2.381402	2.38882	-0.00742
5k	-10	5.172416	0.277487	2.327543	2.348808	-0.02127
5l*	10	-0.26	-0.1022	2.35437	2.422737	-0.06837
5m	-10	15.72511	0.049926	2.283039	2.268521	0.014518
5n*	-10	-0.1772	0.057787	2.306783	2.356267	-0.04948
5o	10	-0.08133	0.018581	2.457942	2.433743	0.024199
5p	5.022896	0.564313	0.104787	2.411165	2.418386	-0.00722
5q	10	-0.40809	0.096589	2.435765	2.443269	-0.0075
5r	10	-0.21852	0.016156	2.4186	2.434253	-0.01565
5s	3.484654	1.079447	0.278161	2.453425	2.426471	0.026954

* Test set compound

3D QSAR

pIC_{50} = 2.3905 + 0.0041 (± 0.82312) E_270–0.0055 (± 0.00022) S_235 + 0.0992 (± 0.05000) E_748 n = 15, r^2 = 0.8921, q^2 = 0.7661, F test = 49.6053……**Model – 2**

The selected model-2 describes the optimum structural features for the anti-inflammatory activity. The descriptors contributing to anti-inflammatory activity as per model-2 are E_270, S_235 and E_748 (Figure 4). The steric field negative at grid point 235 indicates that the steric factor should be lowered to enhance the activity. The electrostatic fields at grid point 270 and 748 are positive indicating necessity of electronegative groups in the second position of aromatic ring attached to 1, 3-thiazolidin-4-one and fourth position of benzamide ring to increase the activity. The 3D descriptors, actual pIC_{50}, predicted pIC_{50} and residual values have been mentioned in Table 4.

Prediction of activity

The predictability of the QSAR model would be good if the values of biological activity predicted by the QSAR model do not appreciably differ from the observed results of biological activity for the given data set. Quality of selected models was further ascertained by r^2, q^2, F test.

CONCLUSION

The anticancer and anti-inflammatory activities of all molecules (5a-5s) suggest that compound 5m is most active in the series. The molecular modeling study also shows that 5m molecule forms most stable complex with PLK1. The present research work shows that 1,3-thiazolidin-4-ones shows anticancer and anti-inflammatory activity. More potent anticancer and anti-inflammatory 1, 3-thiazolidin-4-ones can be generated by substituting the groups as shown in following figure.

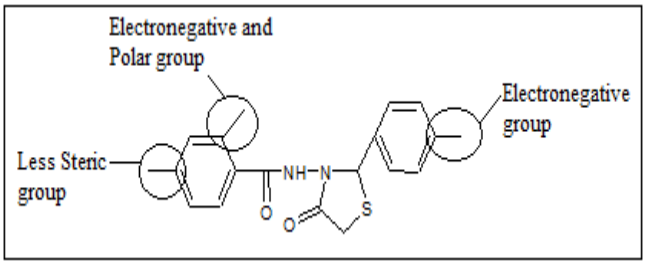

ACKNOWLEDGEMENT

Authors are highly thankful to both college managements for providing us research facilities in the institutes. We are also thankful to Tata Memorial Centre, Navi Mumbai for helping us for anticancer activity.

REFERENCES

1. Singh RK, Singh DP, Tiwari SP, Mohapatra TM. Targeted therapies for cancer treatment. Journal of Pharmacy Research 2011 Feb; 4(2): 312-16.
2. Lee HO, Lee YK, Lee H. 8. Targeting mitotic kinases for anti-cancer treatment. Emerging Signaling Pathways in Tumor Biology; 2010. p. 157.
3. Schöffski P. Polo-like kinase (PLK) inhibitors in preclinical and early clinical development in oncology. Oncologist 2009 Jun 1; 14 (6).
4. Lam FK. Discovery and evaluation of anti-cancer agents (Doctoral dissertation, University of Nottingham).
5. Berridge M. Cell cycle and proliferation. Cell Signalling Biology 2014 Oct 1; 2014(1): 1-45.
6. Bartfeld S. NF-kappaB activation in infections with *Helicobacter pylori* or *Legionella pneumophila.*
7. Schwede W, Schulze V, Eis K, Buchmann B, Briem H, Siemeister G, Boemer U, Parczyk K, inventors; Bayer Pharma AG, assignee. Thiazolidinones and the use therof as polo-like kinase inhibitors. United States patent application US 10/513,368. 2006 Apr 13.
8. Strebhardt K. Multifaceted polo-like kinases: drug targets and anti targets for cancer therapy. Nature reviews Drug discovery 2010 Aug; 9(8): 643-60.
9. Kumar P, Narasimhan B, Sharma D, Judge V, Narang R. Hansch analysis of substituted benzoic acid benzylidene/furan-2-yl-methylene hydrazides as antimicrobial agents. European Journal of Medicinal Chemistry 2009 May 1; 44(5): 1853-63.
10. Husain A, Ahmad A, Alam MM, Ajmal M, Ahuja P. Fenbufen based 3-[5-(substituted aryl)-1, 3, 4-oxadiazol-2-yl]-1-(biphenyl-4-yl) propan-1-ones as safer anti inflammatory and analgesic agents. European Journal of Medicinal Chemistry 2009 Sep 1; 44(9): 3798-804.
11. Visagaperumal D, Kumar RJ, Vijayaraj R, Anbalagan N. Microwave-induced synthesis of some new 3-substituted-1, 3-thiazolidin-4-ones for their potent antimicrobial and anti tubercular activities. International Journal of Chem Tech Research 2009; 4: 1048-51.
12. Kasmi-Mir S, Djafri A, Paquin L, Hamelin J, Rahmouni M. One-pot synthesis of 5-arylidene-2-imino-4-thiazolidinones under microwave irradiation. Molecules 2006 Aug; 11(8): 597-602.
13. Noubade K, Prasad YR, Kumar TV, Patil A, Basawaraj R, Udupi RH. Synthesis and biological activities of thiazolidinones derived from mefenamic acid. Indian Journal of Heterocyclic Chemistry 2009 Oct 1; 19(2): 109-12.
14. Vichai V, Kirtikara K. Sulforhodamine B colorimetric assay for cytotoxicity screening. Nature protocols 2006 Aug; 1(3): 1112.
15. Skehan P, Storeng R, Scudiero D, Monks A, McMahon J, Vistica D, Warren JT, Bokesch H, Kenney S, Boyd MR. New colorimetric cytotoxicity assay for anticancer-drug screening. JNCI: Journal of the National Cancer Institute 1990 Jul 4; 82(13): 1107-12.
16. Singh HP, Sharma CS, Gautam CP. Synthesis and pharmacological screening of some novel 2-arylhydrazino and 2-aryloxy-pyrimido [2, 1-b] benzothiazole derivatives. American-Eurasian Journal of Scientific Research 2009; 4(4): 222-8.
17. Bhaskar VH, Mohite PB. Design, synthesis, characterization and biological evaluation of some novel 1, 5-disubstituted tetrazole as potential anti-inflammatory agents. Journal of optoelectronic and biomedical materials 2010 Oct; 2: 231-7.
18. Molecular Design Suite, V life Sciences Technologies Pvt. Ltd., Pune, India.

19. Halgren TA. Merck molecular force field. III. Molecular geometries and vibration frequencies for MMFF94. Journal of Computational Chemistry 1996 Apr; 17(5-6): 553-86.
20. Baumann K. An alignment-independent versatile structure descriptor for QSAR and QSPR based on the distribution of molecular features. Journal of Chemical Information and Computer Sciences 2002 Jan 28; 42(1): 26-35.
21. Höskuldsson A. A combined theory for PCA and PLS. Journal of Chemometrics 1995 Mar; 9(2): 91-123.

Cite this article as:

Ganesh K. Dhikale *et al*. Microwave assisted Synthesis and Molecular Modeling Studies of Some Novel Polo-like Kinase 1 inhibitors as Anticancer and Anti-inflammatory Agents. Int. Res. J. Pharm. 2020;11(4):56-65 http://dx.doi.org/10.7897/2230-8407.110442

Source of support: Nil, Conflict of interest: None Declared